Research Paper

PAIN®

ACE2 and SCARF expression in human dorsal root ganglion nociceptors: implications for SARS-CoV-2 virus neurological effects

Stephanie Shiers[a], Pradipta R. Ray[a], Andi Wangzhou[a], Ishwarya Sankaranarayanan[a], Claudio Esteves Tatsui[b], Laurence D. Rhines[b], Yan Li[c], Megan L. Uhelski[c], Patrick M. Dougherty[c], Theodore J. Price[a,*]

Abstract

SARS-CoV-2 has created a global crisis. COVID-19, the disease caused by the virus, is characterized by pneumonia, respiratory distress, and hypercoagulation and can be fatal. An early sign of infection is loss of smell, taste, and chemesthesis—loss of chemical sensation. Other neurological effects of the disease have been described, but not explained. It is now apparent that many of these neurological effects (for instance joint pain and headache) can persist for at least months after infection, suggesting a sensory neuronal involvement in persistent disease. We show that human dorsal root ganglion (DRG) neurons express the SARS-CoV-2 receptor, angiotensin-converting enzyme 2 at the RNA and protein level. We also demonstrate that SARS-CoV-2 and coronavirus-associated factors and receptors are broadly expressed in human DRG at the lumbar and thoracic level as assessed by bulk RNA sequencing. *ACE2* mRNA is expressed by a subset of nociceptors that express *MRGPRD* mRNA, suggesting that SARS-CoV-2 may gain access to the nervous system through entry into neurons that form free nerve endings at the outermost layers of skin and luminal organs. Therefore, DRG sensory neurons are a potential target for SARS-CoV-2 invasion of the peripheral nervous system, and viral infection of human nociceptors may cause some of the persistent neurological effects seen in COVID-19.

Keywords: ACE2, MRGPRD, NPPB, Nociceptor, Viral infection, COVID-19

1. Introduction

The SARS-CoV-2 virus that causes COVID-19 enters cells through the angiotensin-converting enzyme 2 (ACE2) receptor. The spike protein of the virus binds to ACE2[32,33] and can be primed by a number of proteases (TMPRSS2[13] and Furin[8]) that are sometimes coexpressed by ACE2-positive cells.[37] A set of genes that are involved in the response to SARS-CoV-2, SARS-CoV-2 and coronavirus-associated factors and receptors (SCARFs),[27] have emerged allowing for assessment of virus effects on tissues through analysis of RNA sequencing or other high-throughput data sets.

Neurological symptoms are common in patients with COVID-19. Loss of smell (anosmia) and taste is an early symptom which is explained by non-neuronal ACE2 expression within the olfactory epithelium.[6] This is sometimes accompanied by loss of chemical sensation, chemesthesis.[21] This chemesthesis includes loss of capsaicin and menthol sensitivity,[21] sensations that are mediated by nociceptive sensory neurons.[4] Other neurological effects of SARS-CoV-2 associated with nociceptors have been described, including headache and nerve pain,[16,18,36] and may be involved in neuro-immune interactions in the lung.[25] Finally, as the pandemic has progressed, it is now clear that many patients do not have a complete recovery from COVID-19 and experience continuing symptoms such as dyspnea, joint pain, chest pain, and cough,[7] all of which are mediated, at least in part, by nociceptors. In addition, severe central nervous system effects such as encephalopathies and delirium have also been observed in patients with COVID-19.[10,22] Molecular mechanisms underlying these effects are not currently known, although studies with human brain organoids demonstrate the ACE2-dependent neuroinvasive potential of the SARS-CoV-2 virus.[28]

Bulk RNA sequencing data sets support the conclusion that *ACE2* is expressed in human DRG,[20,23] but cellular resolution is lacking. Single-cell sequencing experiments from mouse DRG show weak *Ace2* expression in a subset of neurons that also express the *Mrgprd* and *Nppb* genes.[30] MrgprD is selectively expressed in a nociceptor population that forms free nerve endings in the skin,[38] cornea, and luminal organs such as the colon[12] as well as the meninges.[31] We tested the hypothesis that *ACE2* mRNA is expressed in a subset of human DRG neurons using tissues obtained from organ donors or vertebrectomy surgery based on RNAscope in situ hybridization. Our findings support the conclusion that approximately a quarter of human DRG neurons express *ACE2* mRNA and that ACE2 protein is also found in the human DRG. Most of these *ACE2* mRNA–expressing neurons are nociceptors that likely

Sponsorships or competing interests that may be relevant to content are disclosed at the end of this article.

[a] *Department of Neuroscience and Center for Advanced Pain Studies, University of Texas at Dallas, Richardson, TX, United States,* [b] *Department of Neurosurgery, University of Texas MD Anderson Cancer Center, Houston, TX, United States,* [c] *Department of Anesthesia and Pain Medicine, University of Texas MD Anderson Cancer Center, Houston, TX, United States*

**Corresponding author. Address: University of Texas at Dallas, Department of Neuroscience and Center for Advanced Pain Studies, 800 W Campbell RD, BSB 14.102, Richardson TX 75080, United States. E-mail address: Theodore.price@utdallas.edu (T.J. Price).*

Supplemental digital content is available for this article. Direct URL citations appear in the printed text and are provided in the HTML and PDF versions of this article on the journal's Web site (www.painjournalonline.com).

PAIN 161 (2020) 2494–2501

http://dx.doi.org/10.1097/j.pain.0000000000002051

form free nerve endings in skin or other organs, creating a potential entry point for the virus into the peripheral nervous system.

2. Materials and methods

2.1. Tissue preparation

All human tissue procurement procedures were approved by the institutional review boards at the University of Texas at Dallas and University of Texas MD Anderson Cancer Center. Human dorsal root ganglion (DRG) (at levels T4, T5, and L5) was collected, frozen on dry ice (L5) or liquid nitrogen (T4 and T5), and stored in a −80°C freezer. Donor and/or patient information is provided in **Table 1**. The human DRG were gradually embedded with optical coherence tomography in a cryomold by adding small volumes of optical coherence tomography over dry ice to avoid thawing. All tissues were cryostat sectioned at 20 μm onto SuperFrost Plus charged slides. Sections were only briefly thawed to adhere to the slide but were immediately returned to the −20°C cryostat chamber until completion of sectioning. The slides were then immediately used for histology.

2.2. RNAscope in situ hybridization

RNAscope in situ hybridization multiplex version 1 was performed as instructed by Advanced Cell Diagnostics (ACD). Slides were removed from the cryostat and immediately transferred to cold (4°C) 10% formalin for 15 minutes. The tissues were then dehydrated in 50% ethanol (5 minutes), 70% ethanol (5 minutes), and 100% ethanol (10 minutes) at room temperature. The slides were air dried briefly, and then, boundaries were drawn around each section using a hydrophobic pen (ImmEdge PAP pen; Vector Labs, Burlingame, CA). When hydrophobic boundaries had dried, protease IV reagent was added to each section until fully covered and incubated for 5 minutes at room temperature. The protease IV incubation period was optimized as recommended by ACD for the specific lot of protease IV reagent. Slides were washed briefly in 1X phosphate-buffered saline (pH 7.4) at room temperature. Each slide was then placed in a prewarmed humidity control tray (ACD) containing dampened filter paper, and a mixture of channel 1, channel 2, and channel 3 probes (50:1:1 dilution, as directed by ACD due to stock concentrations) was pipetted onto each section until fully submerged. This was performed 1 slide at a time to avoid liquid evaporation and section drying. The humidity control tray was placed in a HybEZ oven (ACD) for 2 hours at 40°C. A table of all probes used is shown in **Table 2**. After probe incubation, the slides were washed 2 times in 1X RNAscope wash buffer and returned to the oven for 30 minutes after submersion in AMP-1 reagent. Washes and amplification were repeated using AMP-2, AMP-3, and AMP-4 reagents with a 15-, 30-, and 15-minute incubation period, respectively. AMP-4 ALT C (channel 1 = Atto 550, channel 2 = Atto 647, and channel 3 = Alexa 488) was used for all experiments. Slides were then washed 2 times in 0.1M phosphate buffer (PB, pH7.4). Human slides were incubated in DAPI (ACD) for 1 minute before being washed, air dried, and coverslipped with ProLong Gold Antifade mounting medium.

2.3. Tissue quality check

All tissues were checked for RNA quality by using a positive control probe cocktail (ACD) which contains probes for high-, medium-, and low-expressing mRNAs that are present in all cells (ubiquitin C > peptidyl-prolyl cis-trans isomerase B > DNA-directed RNA polymerase II subunit RPB1). All tissues showed signal for all 3 positive control probes (Supplementary Fig. 1, available at http://links.lww.com/PAIN/B157). A negative control probe against the bacterial DapB gene (ACD) was used to check for nonspecific/background label.

2.4. Image analysis

Dorsal root ganglion sections were imaged on an Olympus FV3000 confocal microscope at ×20 or ×40 magnification. For the *CALCA/P2RX3/ACE2* and *SCN10A/ACE2* experiments, 3 to 4 20X images were acquired of each human DRG section, and 3 to 4 sections were imaged per human donor. For the *MRGPRD/NPPB/ACE2* experiments, 8 40X images were acquired of each human DRG section, and 3 to 4 sections were imaged per donor. The sections imaged were chosen at random, but preference was given to sections that did not have any sectioning artifact or sections that encompassed the entire DRG bulb. The acquisition parameters were set based on guidelines for the FV3000 provided by Olympus. In particular, the gain was kept at the default setting 1, HV ≤600, offset = 4 (based on HI-LO settings; does not change between experiments), and laser power ≤10% (but generally, the laser power was ≤5% for our experiments). The raw image files were brightened and contrasted in Olympus CellSens software (v1.18) and then analyzed manually 1 cell at a time for expression of each gene target. Cell diameters were measured using the polyline tool. Total neuron counts for human samples were acquired by counting all the probe-labeled neurons and all neurons that were clearly outlined by DAPI (satellite cell) signal and contained lipofuscin in the overlay image.

Large globular structures and/or signal that autofluoresced in all 3 channels (488, 550, and 647; appears white in the 20x RNAscope overlay images) was considered to be background lipofuscin and was not analyzed. Aside from adjusting brightness/contrast, we performed no digital image processing to subtract background. We attempted to optimize automated imaging analysis tools for our purposes, but these tools were designed to work with fresh, low background rodent tissues, not human samples taken from older organ donors. As such, we chose to implement a manual approach in our imaging analysis in which we used our own judgement of the negative/positive controls and target images to assess mRNA label. Images were not analyzed in a blinded fashion.

2.5. Immunohistochemistry

Dorsal root ganglia were sectioned, fixed, and dehydrated as described above. Hydrophobic boundaries were drawn around

Table 1

Human DRG tissue Information.

Donor #	DRG	Sex	Age	Race	Surgery/cause of death	Collection site
1	T4	Male	77	White, non-Hispanic	Vertebrectomy	MD Anderson
2	L5	Female	33	White, non-Hispanic	Opioid overdose	Southwest Transplant Alliance
3	T5	Male	56	White, non-Hispanic	Vertebrectomy	MD Anderson

DRG, dorsal root ganglion.

Table 2

Summary table of Advanced Cell Diagnostics (ACD) RNAscope probes.

mRNA	Gene name	ACD probe cat no.
CALCA	Calcitonin gene-related peptide	605551-C2
P2RX3	Purinergic receptor P2X3	406301-C3
SCN10A	Sodium voltage-gated channel alpha subunit 10; Nav1.8	406291-C2
MRGPRD	MAS-related GPR family member D	524871-C3
NPPB	Natriuretic peptide B	448511-C2
ACE2	Angiotensin –converting enzyme 2	848151-C1

Donor or patient information is given for all the samples that were used for RNAscope in situ hybridization shown in Figure 1.

each section, and then, the slides were submerged in blocking buffer for 1 hour at room temperature. For sections stained using goat ACE2 primary antibody (details below), the blocking buffer was 10% normal donkey serum (Sigma-Aldrich, St Louis, MO; Cat # S30-M), 0.3% Triton X-100 (Sigma-Aldrich; Cat # X100) in 0.1M PB, and for sections stained using rabbit ACE2 primary antibody (details below), the blocking buffer was 10% normal goat serum (Atlanta Biologicals, Flower Branch, GA; Cat # S13150H), 0.3% Triton X-100 in 0.1M PB. Sections were then incubated overnight at 4˚C with one of the following primary antibody cocktails: 1) goat-anti-ACE2 (5 μg/mL; R&D Systems, Minneapolis, MN; AF933; RRID:AB_355722) and rabbit-anti-peripherin (1:1000; Sigma-Aldrich; SAB4502419; RRID: AB_10746677) diluted in donkey serum blocking buffer or 2) rabbit-anti-ACE2 (1:1000; Abcam, Cambridge, United Kingdom; ab15348; RRID:AB_301861) and chicken-anti-peripherin (1:1000; EnCor Biotechnology, Gainsville, FL; CPCA-Peri; RRID:AB_2284443) diluted in goat serum blocking buffer. The next day, sections were washed in 0.1M PB and then incubated in their respective secondary antibody cocktails for 1 hour at room temperature. The secondary antibody cocktails used were 1) donkey-anti-goat H&L 555 (1:2000; Thermo Fisher Scientific; Cat # A-21432; RRID: AB_2535853), donkey-anti-rabbit H&L 488 (1:2000; Thermo Fisher Scientific, San Francisco, CA; Cat# A32790; RRID:AB_2762833), and DAPI (1:5000; Cayman Chemical, Ann Arbor, MI; Cat # 14285) in donkey blocking buffer and 2) goat-anti-rabbit H&L 555 (1:2000; Thermo Fisher Scientific; A21428; RRID:AB_2535849), goat-anti-chicken H&L 488 (1:2000; Thermo Fisher Scientific; A-11039; RRID:AB_2534096), and DAPI (1:5000) in goat blocking buffer. Sections were washed in 0.1M PB, air dried, and coverslipped with ProLong Gold Antifade reagent. Dorsal root ganglion sections were imaged on an Olympus FV3000 confocal microscope at 10X or 40X magnification.

2.6. Western blot

Frozen sections of the lumbar DRG and spinal cord (donor 2) were submerged in lysis buffer (50-mM Tris, pH 7.4, 150-mM NaCl, 1-mM EDTA, pH 8.0, and 1% Triton X-100) containing protease and phosphatase inhibitors (Sigma-Aldrich; Cat #s P8340, P0044, P5726) and then sonicated briefly. Samples were centrifuged at 14,000 rpm for 15 minutes at 4˚C, and the supernatants were transferred to new tubes. Protein concentration was assessed using the Pierce BCA Protein Assay Kit (Thermo Fisher Scientific; Cat # 23225). Ten micrograms of protein was loaded into each lane of a 10% SDS-PAGE gel and then separated using electrophoresis. Proteins were transferred to a 0.45-μm PVDF membrane (Millipore, Burlington, MA) at 30 V overnight at 4˚C. The next day, the membranes were blocked for 1 hour at room temperature. The blocking buffer for the goat-anti-ACE2 antibody was 5% normal donkey serum diluted in 1X Tris buffer solution containing Tween 20 (TTBS), and the blocking buffer used for the rabbit-anti-ACE2 antibody was 5% bovine serum albumin (BSA; Biopharm, Hatfield, AR; Cat # 71-040) in TTBS. Membranes were then incubated in their respective primary antibodies overnight at 4˚C, either goat-anti-ACE2 at 5 μg/mL in donkey blocking buffer or rabbit-anti-ACE2 at 1:1000 in bovine serum albumin blocking buffer. The following day, membranes were washed 3 times in TTBS for 5 minutes each, then incubated with their corresponding secondary antibody, either donkey-anti-goat HRP (1:5000; Jackson ImmunoResearch, West Grove, PA; Cat # 705-035-003) or goat-anti-rabbit HRP (1:10000; Jackson ImmunoResearch; Cat # 111-035-003). Membranes were then washed with TTBS 5 times for 5 minutes each. Signals were detected using Immobilon Western Chemiluminescent HRP substrate (Millipore). Bands were visualized using a Bio-Rad ChemiDoc Touch.

2.7. RNA sequencing sources

We used previously published RNA sequencing data sets to generate **Table 2** and Supplementary file 1 (available at http://links.lww.com/PAIN/B158). Human DRG sequencing data were described previously,[20,23] and mouse single-cell sequencing data from DRG were described previously.[30,34]

2.8. Data analysis

Graphs were generated using GraphPad Prism version 7.01 (GraphPad Software, Inc, San Diego, CA). Given that the percentage of *ACE2*-expressing neurons was assessed in each experiment, we averaged these numbers for each donor to generate the final data values. A total of 2224 neurons were analyzed between all 3 donors and all 3 experiments. A relative frequency distribution histogram with a fitted Gaussian distribution curve was generated using the diameters of all *ACE2*-positive neurons detected in all experiments.

3. Results

We conducted RNAscope for *ACE2* mRNA on human DRG to assess cellular expression of the SARS-CoV-2 receptor. We found that *ACE2* mRNA was localized to some neurons, many of which expressed calcitonin gene-related peptide gene, *CALCA* (**Figs. 1A and B**), and/or the P2X purinergic ion channel type 3 receptor gene, *P2RX3*. Both *CALCA* and *P2RX3* have been

widely used to delineate nociceptor subpopulations in rodent DRG.[4] Expression of *ACE2* was consistent in lumbar DRG from a female organ donor (**Table 2**, demographic data for all DRG analyzed) and in 2 thoracic DRG taken from male patients undergoing vertebrectomy surgery (**Fig. 1B**). Across samples, *ACE2* mRNA was present in 19.8 to 25.4% of all sensory neurons (**Fig. 1C**); however, mRNA puncta for *ACE2* was sparse, suggesting a low level of expression. Consistent with mouse single-cell RNA sequencing data, *ACE2* neurons coexpressed *MRGPRD* and *NPPB mRNA* (**Fig. 1D**). They also coexpressed Nav1.8 (*SCN10A* gene) mRNA (**Fig. 1E**). *SCN10A* is a nociceptor-specific marker in rodent DRG at the protein and mRNA levels[1,9,26]; therefore, these findings are consistent with the notion that *ACE2* mRNA is mostly expressed by nociceptors

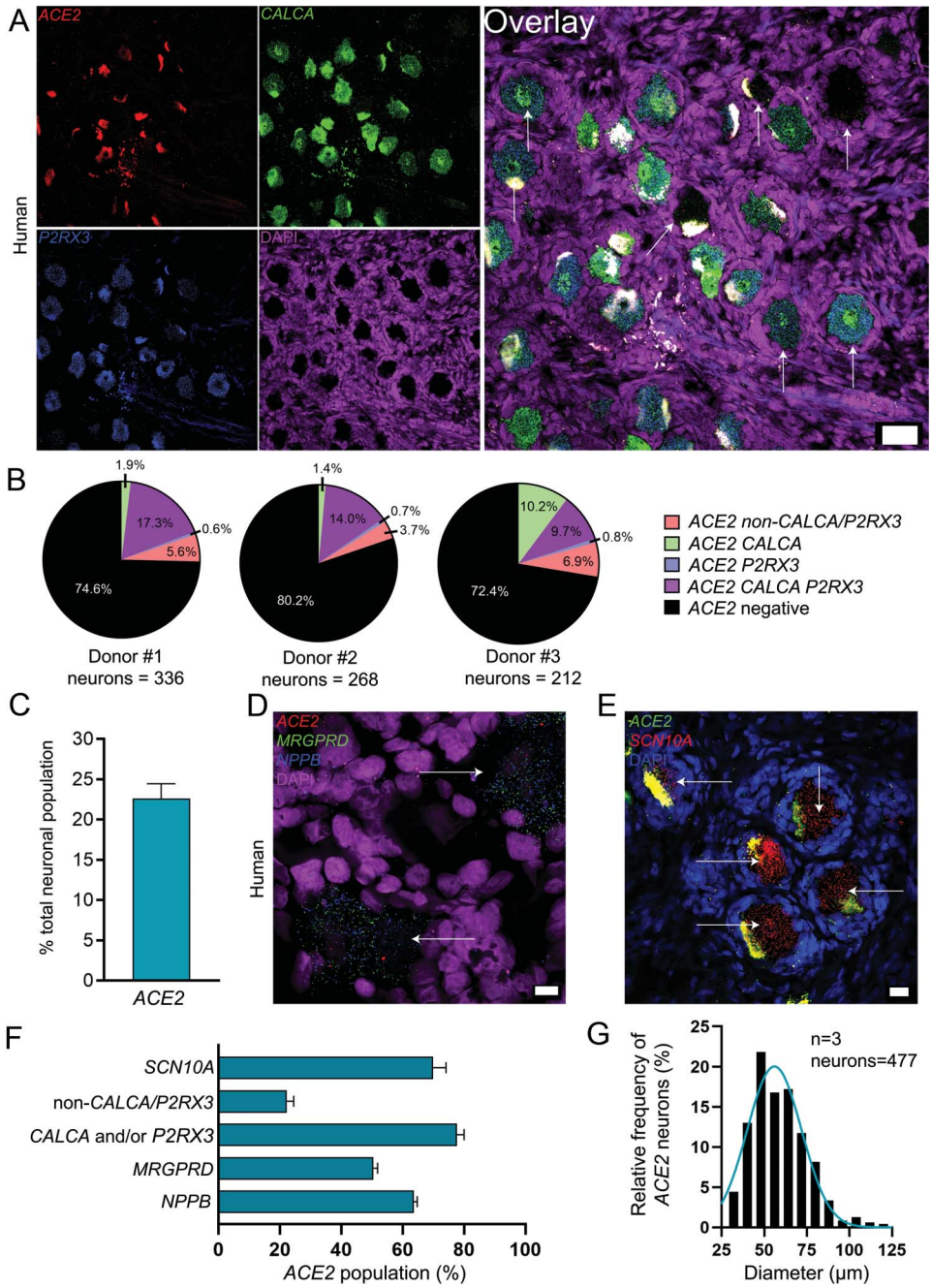

Figure 1. Distribution of *ACE2* mRNA in human dorsal root ganglia (DRG). (A) Representative 20x images of human DRG labeled with RNAscope in situ hybridization for *CALCA* (green), *P2RX3* (blue), and *ACE2* (red) mRNA and costained with DAPI (purple). Lipofuscin (globular structures) that autofluoresced in all 3 channels and appear white in the overlay image were not analyzed as this is background signal that is present in all human nervous tissue. (B) Pie charts showing distribution of *ACE2* neuronal subpopulations for each human donor DRG. *ACE2* was found in neurons expressing solely *CALCA* (green), solely *P2RX3* (blue), or both (purple) and a smaller population of neurons negative for both *CALCA* and *P2RX3* (red). Some mRNA was detected in non-neuronal cells that are likely vascular or satellite glia but not immune cells (Supplementary file 1, available at http://links.lww.com/PAIN/B158). (C) *ACE2* was expressed in 22.6% of all sensory neurons in human DRG. (D) Representative 100x overlay image showing *MRGPRD* (green), *NPPB* (blue), *ACE2* (red), and DAPI (purple) signal in human DRG. (E) Representative 40x overlay image showing *SCN10A* (blue), *ACE2* (red), and DAPI (purple) signal in human DRG. (F) Approximately 69.9% of *ACE2* neurons expressed *SCN10A*, 77.7% expressed *CALCA* and/or *P2RX3*, 22.2% were negative for *CALCA* and/or *P2RX3*, 50.4% expressed *MRGPRD*, and 63.6% expressed *NPPB*. (G) Size distribution of *ACE2* mRNA positive neurons. Scale bars: 20x = 50 μm, 40x = 20 μm, 100x = 10 μm. White arrows point toward *ACE2*-positive neurons.

in the human DRG. Summary statistics for the ACE2 population and *ACE2* mRNA-positive neuron cell sizes are shown in **Figures 1F and G**.

We next investigated whether ACE2 protein was present in human DRG. We conducted immunohistochemistry and western blot analysis of human lumbar and thoracic DRG using 2 commercially available ACE2 antibodies (Abcam ab15348 and R&D Systems AF933) which are both extensively cited (see product datasheets for publication lists) and recently used in several SARS-CoV-2–related research articles.[13,15,19,28,35] It is important to note that these antibodies are both polyclonals and have not been knockout validated; therefore, their reliability as ACE2-specific markers is unverified using mouse gene knockout. To the best of our knowledge, no commercial ACE2 antibody has been validated for specificity in human tissue. We observed similar protein staining for both antibodies in both lumbar and thoracic human DRG which was found in both neurons and non-neuronal cells including some satellite glial cells (**Figs. 2A–C**; and Supplementary Figs. 2A–C, available at http://links.lww.com/PAIN/B157). Both antibodies gave several nonspecific bands on a western blot; however, a band at the predicted molecular weight for ACE2 was observed for both antibodies (**Fig 2D**; and Supplementary Fig. 2D, available at http://links.lww.com/PAIN/B157). The western blot signal for ab15348 was cleaner and matched the expected differential expression of ACE2 between the human spinal cord and DRG in which the mRNA is virtually undetectable in the spinal cord,[17,24] but present in DRG (**Fig. 1**). These findings support the notion that ACE2 protein is found in human DRG where it is likely secreted, binding to membranes of surrounding cells, as observed in human brain organoids.[2,28]

Having established that the major receptor for SARS-CoV-2 is likely expressed by a specific subset of human nociceptors, we sought to use existing sequencing data sets to assess expression of other SCARFs[27] in human DRG. We grouped these into receptors, proteases, replication factors, trafficking factors (shown only in supplementary file 1, available at http://links.lww.com/PAIN/B158, because they were all ubiquitous), and restriction factors (**Table 3**; and supplementary file 1, available at http://links.lww.com/PAIN/B158) as described in other surveys of RNA sequencing databases, none of which included DRG. Although *ACE2* expression is low in these bulk RNA sequencing data sets, it was reliably detectable above 1 transcript per million in certain thoracic DRG samples (Supplementary file 1, available at http://links.lww.com/PAIN/B158). Some other potential receptors for SARS and MERS viruses were also found in human DRG and expressed in mouse DRG neurons, suggesting they may also be neuronally expressed in human DRG. Among proteases, the 2 main proteases for the SARS-CoV-2 spike protein priming, *TMPRSS2* and *FURIN*, were robustly expressed in human DRG, and they were also expressed by mouse DRG neurons (**Table 3**). Most other SCARFs were also expressed in human DRG, and, again, their expression in mouse DRG neurons suggests that most of them are likely to also be found in human DRG neurons. Many of these genes showed high variation between samples, an effect that may explain variable effects of SARS-CoV-2 on the nervous system in patients.

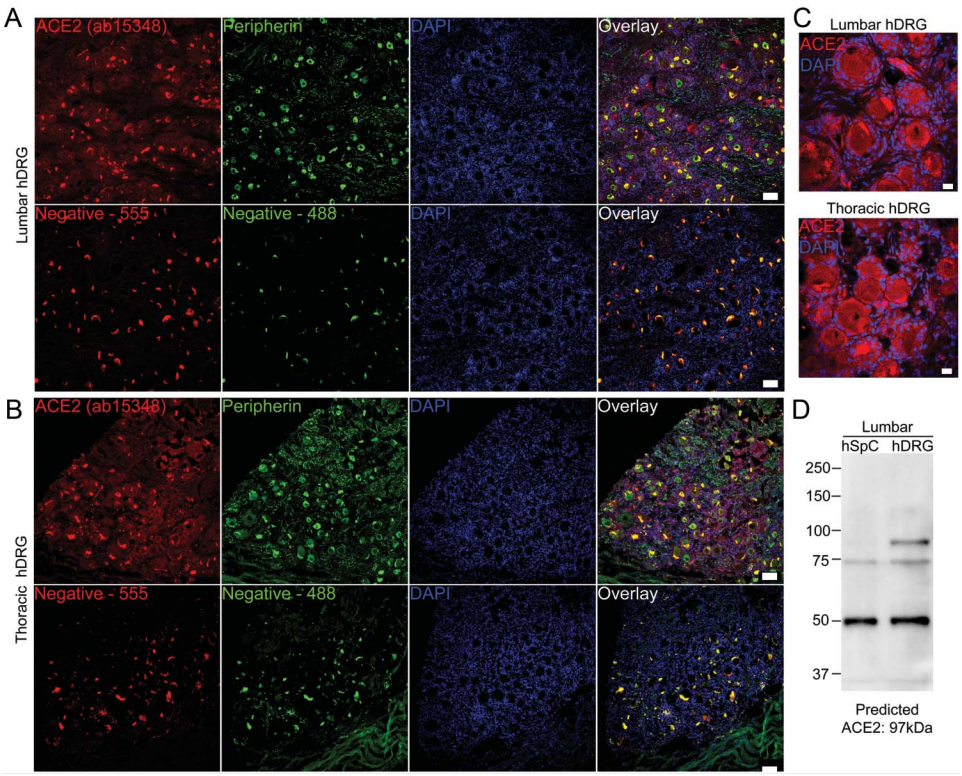

Figure 2. ACE2 protein is detected in human dorsal root ganglia (DRG) using the Abcam ab15348 antibody. (A) Representative 10x images of protein staining for ACE2 (red; Abcam ab15348), peripherin (green; a sensory neuron marker), and DAPI (blue) in lumbar and (B) thoracic human DRG. (C) 40x images showing ACE2 signal in both neurons and non-neuronal cells including satellite glial cells. (D) Western blot of ACE2 using ab15348 on the lumbar spinal cord and DRG revealed a strong band at the predicted molecular weight of ACE2 protein in human DRG but not the spinal cord and other nonspecific bands. Scale bars: 10x = 100 μm, 40x = 20 μm. hDRG, human dorsal root ganglion; hSpC, human spinal cord.

Table 3

Expression of SCARF genes in human DRG from bulk RNA sequencing experiments.

Human gene	Lumbar DRG (mean ± SD) TPM	Thoracic DRG (mean ± SD) TPM	Neuronal expression in mouse DRG?	SCARF classification
ACE2	0.09 ± 0.02	0.94 ± 0.88	NF	Receptors
BSG	304.82 ± 82.3	239.42 ± 79.23	PEP, NP, NF, and TH	Receptors
ANPEP	14.56 ± 7.27	13.73 ± 4.26	PEP and TH	Receptors
CD209	0.57 ± 0.43	1.60 ± 1.28	Multiple mouse orthologs	Receptors
CLEC4G	0.79 ± 0.34	0.22 ± 0.45	ND	Receptors
CLEC4M	0.02 ± 0.03	0.19 ± 0.17	No ortholog	Receptors
DPP4	0.34 ± 0.23	3.75 ± 4.05	ND	Receptors
TMPRSS2	3.05 ± 1.04	6.69 ± 2.65	NF and TH	Proteases
TMPRSS11A	ND	0.06 ± 0.13	NF and TH	Proteases
TMPRSS11B	ND	0.03 ± 0.04	No ortholog	Proteases
FURIN	20.86 ± 5.69	34.11 ± 10.44	PEP, NP, NF, and TH	Proteases
TMPRSS4	0.77 ± 0.30	0.08 ± 0.09	NF	Proteases
CTSL	154.53 ± 21.71	105.19 ± 13.36	PEP, NP, NF, and TH	Proteases
CTSB	1116.17 ± 132.45	697.50 ± 96.96	PEP, NP, NF, and TH	Proteases
TOP3B	6.46 ± 0.88	18.93 ± 5.45	PEP, NP, NF, and TH	Replication factors
MADP1	35.13 ± 8.08	32.74 ± 7.44	PEP, NP, NF, and TH	Replication factors
LY6E	446.65 ± 234.34	218.17 ± 161.15	PEP, NP, NF, and TH	Restriction factors
IFITM1	828.53 ± 425.04	322.86 ± 104.16	PEP, NP, NF, and TH	Restriction factors
IFITM2	880.05 ± 340.01	2241.85 ± 91.24	PEP, NP, NF, and TH	Restriction factors
IFITM3	2339.37 ± 943.43	744.00 ± 224.85	PEP, NP, NF, and TH	Restriction factors
CALCA	1634.46 ± 665.44	524.86 ± 111.60	PEP, NP, NF, and TH	Neuronal markers
P2RX3	44.65 ± 42.69	144.54 ± 47.60	PEP, NP, NF, and TH	Neuronal markers
NPPB	41.20 ± 16.37	21.29 ± 8.99	NP and PEP	Neuronal markers
MRGPRD	3.01 ± 4.62	10.47 ± 7.64	PEP, NP, NF, and TH	Neuronal markers

Genes are shown with mean ± SD expression in TPMs in 3 lumbar DRG samples and 5 thoracic DRG samples. Mouse DRG neuronal expression denotes detection in the neurofilament (NF), peptidergic (PEP), nonpeptidergic (NP), and tyrosine hydroxylase (TH) subsets of DRG neurons. Human DRG data are from Refs. 20 and 23, and mouse single-cell data are from Ref. 30.
DRG, dorsal root ganglion; ND, not detectable; SCARF, SARS-CoV-2 and coronavirus-associated factors and receptor; TPM, transcript per million.

4. Discussion

Our work highlights neuronal expression of *ACE2* in a select subset of nociceptors that express *CALCA*, *P2RX3*, *MRGPRD*, *NPPB*, and *SCN10A*. Although we cannot state with certainty the anatomical projections of these neurons because tracing studies cannot be performed in humans, the neurochemical signature of these neurons is consistent with nociceptors that form free nerve endings in the skin,[38] luminal organs,[12] and meninges.[31] Therefore, 1 potential consequence of this ACE2 expression could be infection of nociceptors through the nasal passages, cornea, or upper or lower airway. To this end, we noted higher expression of *ACE2* in thoracic DRG, and these DRG contain nociceptors that innervate the lungs,[14,29] a major site for proliferation of the SARS-CoV-2 virus.[36] It is now clear that many patients with COVID-19 have persistent symptoms lasting for months after initial infection. These symptoms include joint and chest pain, cough, headache, and dyspnea,[7] symptoms that involve activation of nociceptors. Sensory neuronal infection by SARS-CoV-2 may be a causative factor in some of these persistent symptoms.

An interesting early symptom of SARS-CoV-2 is chemesthesis.[21] This symptom is less frequent than loss of smell and cannot be explained through the same mechanisms as anosmia[5] because the sensing of noxious chemicals in the oral cavity is mediated by nociceptors. Our data suggest that a possible explanation of chemesthesis in COVID-19 is silencing of nerve endings by the initial viral infection. If pulmonary afferents are also infected by SARS-CoV-2, as our data would predict, this could have important consequences for disease severity. Previous studies have shown that ablation of airway nociceptors increases the severity of respiratory disease due to a loss of the trophic action of CGRP within the airway.[3] Widespread, early silencing of nociceptors innervating the oral and nasal cavity as well as the upper and lower airway may have important impacts on COVID-19 disease severity.

There are many currently unexplained neurological features in patients with COVID-19,[16,18] including persistent symptoms such as joint pain and headache linked to nociceptor function.[7] It is mysterious how the virus enters the nervous system as most neurons do not express ACE2.[11,27] Our work presents a plausible entry point for the peripheral nervous system—through a select subset of ACE2-expressing nociceptors. Although our findings can be taken as putative evidence for this idea, *ACE2* mRNA expression is very low in these neurons, and we have not tested whether ACE2 protein can be detected in free nerve endings in appropriate organs, or whether such expression can be harnessed by the virus to gain entry. We did observe ACE2

protein expression within the human DRG. Studies in brain organoids demonstrate that SARS-CoV-2 can infect neurons, and the virus does so in an ACE2-dependent fashion.[28] Interestingly, ACE2 mRNA expression is low in human brain organoids, but this low mRNA expression leads to widespread ACE2 protein staining within the organoids.[28] We obtained similar results using 2 independent antibodies, one of which was used in the brain organoid study.[28] Therefore, our results in human DRG are consistent with the idea that low-level mRNA expression can lead to broader protein expression likely because ACE2 is a secreted protein that is bound to the extracellular part of the cellular plasma membrane.[2] This finding, coupled with the strong expression of many SCARFs in human DRG, suggests that sensory neurons can be targeted by SARS-CoV-2.

More work will be needed to better understand the impact of SARS-CoV-2 on nociceptors. Our results lay a foundation for beginning to understand the symptoms, pathology, and long-term outcomes of COVID-19 as they relate to the sensory nervous system. As this pandemic continues to spread, it will be important to study these neurobiological findings in the context of long-term patient outcomes, in particular as they relate to pain and other forms of chemosensation that rely on nociceptors.

Conflict of interest statement

The authors have no conflicts of interest to declare.

Acknowledgements

The work was funded by NIH grants NS111929 to P.M. Dougherty and T.J. Price and NS065926 to T.J. Price. The UTD authors dedicate this work to the memory of our friend and colleague Zhiyue "Mark" Wang. The authors are grateful to the patients and the families of organ donors who provided the DRG for this study. Human DRG nociceptors, including neurons that also express MRGPRD, express the SARS-CoV-2 virus receptor ACE2.

Appendix A. Supplemental digital content

Supplemental digital content associated with this article can be found online at http://links.lww.com/PAIN/B157 and http://links.lww.com/PAIN/B158.

Article history:
Received 16 June 2020
Received in revised form 15 July 2020
Accepted 27 July 2020
Available online 18 August 2020

References

[1] Akopian AN, Sivilotti L, Wood JN. A tetrodotoxin-resistant voltage-gated sodium channel expressed by sensory neurons. Nature 1996;379:257–62.
[2] Antalis TM, Conway GD, Peroutka RJ, Buzza MS. Membrane-anchored proteases in endothelial cell biology. Curr Opin Hematol 2016;23:243–52.
[3] Baral P, Umans BD, Li L, Wallrapp A, Bist M, Kirschbaum T, Wei Y, Zhou Y, Kuchroo VK, Burkett PR, Yipp BG, Liberles SD, Chiu IM. Nociceptor sensory neurons suppress neutrophil and gammadelta T cell responses in bacterial lung infections and lethal pneumonia. Nat Med 2018;24:417–26.
[4] Basbaum AI, Bautista DM, Scherrer G, Julius D. Cellular and molecular mechanisms of pain. Cell 2009;139:267–84.
[5] Brann DH, Tsukahara T, Weinreb C, Lipovsek M, Van den Berge K, Gong B, Chance R, Macaulay IC, Chou H-j, Fletcher R, Das D, Street K, de Bezieux HR, Choi Y-G, Risso D, Dudoit S, Purdom E, Mill JS, Hachem RA, Matsunami H, Logan DW, Goldstein BJ, Grubb MS, Ngai J, Datta SR. Non-neuronal expression of SARS-CoV-2 entry genes in the olfactory system suggests mechanisms underlying COVID-19-associated anosmia. Science Advances 2020;6:1–19.
[6] Butowt R, Bilinska K. SARS-CoV-2: olfaction, brain infection, and the urgent need for clinical samples allowing earlier virus detection. ACS Chem Neurosci 2020;11:1200–3.
[7] Carfi A, Bernabei R, Landi F; Gemelli Against C-P-ACSG. Persistent symptoms in patients after acute COVID-19. JAMA 2020;324:603–5.
[8] Coutard B, Valle C, de Lamballerie X, Canard B, Seidah NG, Decroly E. The spike glycoprotein of the new coronavirus 2019-nCoV contains a furin-like cleavage site absent in CoV of the same clade. Antivir Res 2020;176:104742.
[9] Dib-Hajj SD, Tyrrell L, Cummins TR, Black JA, Wood PM, Waxman SG. Two tetrodotoxin-resistant sodium channels in human dorsal root ganglion neurons. FEBS Lett 1999;462:117–20.
[10] Hernandez-Fernandez F, Valencia HS, Barbella-Aponte RA, Collado-Jimenez R, Ayo-Martin O, Barrena C, Molina-Nuevo JD, Garcia-Garcia J, Lozano-Setien E, Alcahut-Rodriguez C, Martinez-Martin A, Sanchez-Lopez A, Segura T. Cerebrovascular disease in patients with COVID-19: neuroimaging, histological and clinical description. Brain 2020. doi: 10.1093/brain/awaa239 [Epub ahead of print].
[11] Hikmet F, Méar L, Edvinsson Å, Micke P, Uhlén M, Lindskog C. The protein expression profile of ACE2 in human tissues. Mol Syst Biol 2020;16:e9610.
[12] Hockley JRF, Taylor TS, Callejo G, Wilbrey AL, Gutteridge A, Bach K, Winchester WJ, Bulmer DC, McMurray G, Smith ESJ. Single-cell RNAseq reveals seven classes of colonic sensory neuron. Gut 2018;68:633–44.
[13] Hoffmann M, Kleine-Weber H, Schroeder S, Kruger N, Herrler T, Erichsen S, Schiergens TS, Herrler G, Wu NH, Nitsche A, Muller MA, Drosten C, Pohlmann S. SARS-CoV-2 cell entry depends on ACE2 and TMPRSS2 and is blocked by a clinically proven protease inhibitor. Cell 2020;181:271–80.e278.
[14] Kummer W, Fischer A, Kurkowski R, Heym C. The sensory and sympathetic innervation of Guinea-pig lung and trachea as studied by retrograde neuronal tracing and double-labelling immunohistochemistry. Neuroscience 1992;49:715–37.
[15] Leung JM, Yang CX, Tam A, Shaipanich T, Hackett TL, Singhera GK, Dorscheid DR, Sin DD. ACE-2 expression in the small airway epithelia of smokers and COPD patients: implications for COVID-19. Eur Respir J 2020;55:2000688.
[16] Mao L, Jin H, Wang M, Hu Y, Chen S, He Q, Chang J, Hong C, Zhou Y, Wang D, Miao X, Li Y, Hu B. Neurologic manifestations of hospitalized patients with coronavirus disease 2019 in Wuhan, China. JAMA Neurol 2020;77:1–9.
[17] Mele M, Ferreira PG, Reverter F, DeLuca DS, Monlong J, Sammeth M, Young TR, Goldmann JM, Pervouchine DD, Sullivan TJ, Johnson R, Segre AV, Djebali S, Niarchou A, Consortium GT, Wright FA, Lappalainen T, Calvo M, Getz G, Dermitzakis ET, Ardlie KG, Guigo R. Human genomics. The human transcriptome across tissues and individuals. Science 2015;348:660–5.
[18] Montalvan V, Lee J, Bueso T, De Toledo J, Rivas K. Neurological manifestations of COVID-19 and other coronavirus infections: a systematic review. Clin Neurol Neurosurg 2020;194:105921.
[19] Nicin L, Abplanalp WT, Mellentin H, Kattih B, Tombor L, John D, Schmitto JD, Heineke J, Emrich F, Arsalan M, Holubec T, Walther T, Zeiher AM, Dimmeler S. Cell type-specific expression of the putative SARS-CoV-2 receptor ACE2 in human hearts. Eur Heart J 2020;41:1804–6.
[20] North RY, Li Y, Ray P, Rhines LD, Tatsui CE, Rao G, Johansson CA, Zhang H, Kim YH, Zhang B, Dussor G, Kim TH, Price TJ, Dougherty PM. Electrophysiological and transcriptomic correlates of neuropathic pain in human dorsal root ganglion neurons. Brain 2019;142:1215–26.
[21] Parma V, Ohla K, Veldhuizen MG, Niv MY, Kelly CE, Bakke AJ, Cooper KW, Bouysset C, Pirastu N, Dibattista M, Kaur R, Liuzza MT, Pepino MY, Schöpf V, Pereda-Loth V, Olsson SB, Gerkin RC, Domínguez PR, Albayay J, Farruggia MC, Bhutani S, Fjaeldstad AW, Kumar R, Menini A, Bensafi M, Sandell M, Konstantinidis I, Di Pizio A, Genovese F, Öztürk L, Thomas-Danguin T, Frasnelli J, Boesveldt S, Ö Saatci, Saraiva LR, Lin C, Golebiowski J, Hwang LD, Ozdener MH, Guàrdia MD, Laudamiel C, Ritchie M, Havlícek J, Pierron D, Roura E, Navarro M, Nolden AA, Lim J, Whitcroft K, Colquitt LR, Ferdenzi C, Brindha EV, Altundag A, Macchi A, Nunez-Parra A, Patel ZM, Fiorucci S, Philpott CM, Smith BC, Lundström JN, Mucignat C, Parker JK, van den Brink M, Schmuker M, Fischmeister FPS, Heinbockel T, Shields VDC, Faraji F, Enrique Santamaría E, Fredborg WEA, Morini G, Olofsson JK, Jalessi M, Karni N, D'Errico A, Alizadeh R, Pellegrino R, Meyer P, Huart C, Chen B, Soler GM, Alwashahi MK, Abdulrahman O, Welge-Lüssen A, Dalton P, Freiherr J, Yan CH, de Groot JHB, Voznessenskaya VV, Klein H, Chen J, Okamoto M, Sell EA, Singh PB, Walsh-Messinger J, Archer NS, Koyama S, Deary V, Roberts

SC, Yanik H, Albayrak S, Novákov LM, Croijmans I, Mazal PP, Moein ST, Margulis E, Mignot C, Mariño S, Georgiev D, Kaushik PK, Malnic B, Wang H, Seyed-Allaei S, Yoluk N, Razzaghi S, Justice JM, Restrepo D, Hsieh JW, Reed DR, Hummel T, Munger SD, Hayes JE; GCCR Group Author. More Than Smell—COVID-19 Is Associated With Severe Impairment of Smell, Taste, and Chemesthesis Chemical Senses 2020. doi: 10.1093/chemse/bjaa041 [Epub ahead of print].

[22] Paterson RW, Brown RL, Benjamin L, Nortley R, Wiethoff S, Bharucha T, Jayaseelan DL, Kumar G, Raftopoulos RE, Zambreanu L, Vivekanandam V, Khoo A, Geraldes R, Chinthapalli K, Boyd E, Tuzlali H, Price G, Christofi G, Morrow J, McNamara P, McLoughlin B, Lim ST, Mehta PR, Levee V, Keddie S, Yong W, Trip SA, Foulkes AJM, Hotton G, Miller TD, Everitt AD, Carswell C, Davies NWS, Yoong M, Attwell D, Sreedharan J, Silber E, Schott JM, Chandratheva A, Perry RJ, Simister R, Checkley A, Longley N, Farmer SF, Carletti F, Houlihan C, Thom M, Lunn MP, Spillane J, Howard R, Vincent A, Werring DJ, Hoskote C, Jager HR, Manji H, Zandi MS; UCLQSNHf Neurology, Neurosurgery CSG. The emerging spectrum of COVID-19 neurology: clinical, radiological and laboratory findings. Brain 2020. doi: 10.1093/brain/awaa240 [Epub ahead of print].

[23] Ray P, Torck A, Quigley L, Wangzhou A, Neiman M, Rao C, Lam T, Kim JY, Kim TH, Zhang MQ, Dussor G, Price TJ. Comparative transcriptome profiling of the human and mouse dorsal root ganglia: an RNA-seq-based resource for pain and sensory neuroscience research. PAIN 2018;159:1325–45.

[24] Ray PR, Khan J, Wangzhou A, Tavares-Ferreira D, Akopian AN, Dussor G, Price TJ. Transcriptome analysis of the human tibial nerve identifies sexually dimorphic expression of genes involved in pain, inflammation, and neuro-immunity. Front Mol Neurosci 2019;12:37.

[25] Ray PR, Wangzhou A, Ghneim N, Yousuf MS, Paige C, Tavares-Ferreira D, Mwirigi JM, Shiers S, Sankaranarayanan I, McFarland AJ, Neerukonda SV, Davidson S, Dussor G, Burton MD, Price TJ. A pharmacological interactome between COVID-19 patient samples and human sensory neurons reveals potential drivers of neurogenic pulmonary dysfunction. Brain Behav Immun 2020. doi: 10.1016/j.bbi.2020.05.078 [Epub ahead of print].

[26] Sangameswaran L, Delgado SG, Fish LM, Koch BD, Jakeman LB, Stewart GR, Sze P, Hunter JC, Eglen RM, Herman RC. Structure and function of a novel voltage-gated, tetrodotoxin-resistant sodium channel specific to sensory neurons. J Biol Chem 1996;271:5953–6.

[27] Singh M, Bansal V, Feschotte C. A single-cell RNA expression map of human coronavirus entry factors. bioRxiv 2020. doi: 10.1101/2020.05.08.084806.

[28] Song E, Zhang C, Israelow B, Lu P, Weizman OE, Liu F, Dai Y, Szigeti-Buck K, Yasumoto Y, Wang G, Castaldi C, Heltke J, Ng E, Wheeler J, Alfajaro MM, Fontes B, Ravindra NG, Van Dijk D, Mane S, Gunel M, Ring A, Wilen CB, Horvath TL, Louvi A, Farhadian SF, Bilguvar K, Iwasaki A. Neuroinvasive potential of SARS-CoV-2 revealed in a human brain organoid model. bioRxiv 2020. doi: 10.1101/2020.06.25.169946.

[29] Springall DR, Cadieux A, Oliveira H, Su H, Royston D, Polak JM. Retrograde tracing shows that CGRP-immunoreactive nerves of rat trachea and lung originate from vagal and dorsal root ganglia. J Auton Nerv Syst 1987;20:155–66.

[30] Usoskin D, Furlan A, Islam S, Abdo H, Lonnerberg P, Lou D, Hjerling-Leffler J, Haeggstrom J, Kharchenko O, Kharchenko PV, Linnarsson S, Ernfors P. Unbiased classification of sensory neuron types by large-scale single-cell RNA sequencing. Nat Neurosci 2015;18:145–53.

[31] von Buchholtz LJ, Lam RM, Emrick JJ, Chesler AT, Ryba NJP. Assigning transcriptomic class in the trigeminal ganglion using multiplex in situ hybridization and machine learning. PAIN 2020;161:2212–24.

[32] Wan Y, Shang J, Graham R, Baric RS, Li F. Receptor recognition by the novel coronavirus from Wuhan: an analysis based on decade-long structural studies of SARS coronavirus. J Virol 2020;94:e00127–20.

[33] Yan R, Zhang Y, Li Y, Xia L, Guo Y, Zhou Q. Structural basis for the recognition of SARS-CoV-2 by full-length human ACE2. Science 2020;367:1444–8.

[34] Zeisel A, Hochgerner H, Lonnerberg P, Johnsson A, Memic F, van der Zwan J, Haring M, Braun E, Borm LE, La Manno G, Codeluppi S, Furlan A, Lee K, Skene N, Harris KD, Hjerling-Leffler J, Arenas E, Ernfors P, Marklund U, Linnarsson S. Molecular architecture of the mouse nervous system. Cell 2018;174:999–1014.e1022.

[35] Zhao X, Chen D, Szabla R, Zheng M, Li G, Du P, Zheng S, Li X, Song C, Li R, Guo J-T, Junop M, Zeng H, Lin H. Broad and differential animal ACE2 receptor usage by SARS-CoV-2. Journal of Virology 2020. 10.1128/JVI.00940-20.

[36] Zhou F, Yu T, Du R, Fan G, Liu Y, Liu Z, Xiang J, Wang Y, Song B, Gu X, Guan L, Wei Y, Li H, Wu X, Xu J, Tu S, Zhang Y, Chen H, Cao B. Clinical course and risk factors for mortality of adult inpatients with COVID-19 in Wuhan, China: a retrospective cohort study. Lancet 2020;395:1054–62.

[37] Ziegler CGK, Allon SJ, Nyquist SK, Mbano IM, Miao VN, Tzouanas CN, Cao Y, Yousif AS, Bals J, Hauser BM, Feldman J, Muus C, Wadsworth MH II, Kazer SW, Hughes TK, Doran B, Gatter GJ, Vukovic M, Taliaferro F, Mead BE, Guo Z, Wang JP, Gras D, Plaisant M, Ansari M, Angelidis I, Adler H, Sucre JMS, Taylor CJ, Lin B, Waghray A, Mitsialis V, Dwyer DF, Buchheit KM, Boyce JA, Barrett NA, Laidlaw TM, Carroll SL, Colonna L, Tkachev V, Peterson CW, Yu A, Zheng HB, Gideon HP, Winchell CG, Lin PL, Bingle CD, Snapper SB, Kropski JA, Theis FJ, Schiller HB, Zaragosi LE, Barbry P, Leslie A, Kiem HP, Flynn JL, Fortune SM, Berger B, Finberg RW, Kean LS, Garber M, Schmidt AG, Lingwood D, Shalek AK, Ordovas-Montanes J; HCALBNEa, Network HCALB. SARS-CoV-2 receptor ACE2 is an interferon-stimulated gene in human airway epithelial cells and is detected in specific cell subsets across tissues. Cell 2020;181:1016–35.

[38] Zylka MJ, Rice FL, Anderson DJ. Topographically distinct epidermal nociceptive circuits revealed by axonal tracers targeted to Mrgprd. Neuron 2005;45:17–25.